Observation and model of highly ordered wavy cracks due to coupling of in-plane stress and interface debonding in silica thin films

Neng Wan (万能), Jun Xu (徐骏),* Tao Lin (林涛), Ling Xu (徐岭), and Kunji Chen (陈坤基)
Department of Physics and Nanjing National Laboratory of Microstructures, Nanjing University, Nanjing 210093, People's Republic of China

(Received 23 January 2009; revised manuscript received 3 July 2009; published 31 July 2009)

Highly ordered wavy cracks are observed in silica films deposited on crystalline Si wafer. The wavy crack path is interpreted in terms of the coupling of the in-plane film crack and the interface debonding. A model based on the analyzing of the crack path and the stress evolution is proposed to describe the propagation of the wavy cracks. A scaling relationship between the wavelength (λ) and amplitude (A) is found ($\lambda \sim A^{\xi}$) and the scaling factor is determined to be $\xi = 0.47 \pm 0.01$.

DOI: 10.1103/PhysRevB.80.014121 PACS number(s): 62.20.mm, 46.50.+a, 89.75.Da, 89.75.Kd

I. INTRODUCTION

It is a general problem to understand the formation and propagation of cracks of materials because of its importance both in fundamental research and applications in many fields.[1–3] Although enormous effects have been made in understanding the stability of cracks, prediction of the cracks path still remains an open question. Fascinating crack patterns have been observed recently in several kinds of systems which have attracted extensive research interests. For example, Yuse *et al.* reported the highly ordered cracks when quenching a strip of heated glass in well-controlled conditions.[4] The cracks have sinusoidal, semicircle, or asymmetric shapes with wavelength around several centimeters. This report stimulated numerable theoretical, experimental, and numerical studies up to now.[5–8] It is found that the crack trajectory can be simulated and interpreted by using the phase-field model.[9] More recently, the similar oscillatory crack was observed when a rigid rod was forced through a thin polymer film and tears through the material as it advanced. It was found that the wavelength and the amplitude of the crack, which was later realized to be ruled by the geometry, are dependent on the diameter of the rod.[10] Meantime, the spiral and curved crack patterns were also observed in the silica films deposited on substrate by sol-gel method,[11] and cracks with different morphology, such as crescent periodic cracks, saw-tooth cracks, and conical spiral cracks can be observed. Unfortunately, although detailed descriptions have been given on the cracks, the physical explanation is still lacking for further understanding this interesting phenomenon.

The study about the failure of the thin films deposited on substrate has been drawn much attention, especially on the silica films deposited on crystalline silicon wafers, which is one of the most important heterostructures in microelectronic devices. Different with the freestanding system, films deposited on substrate have some unique characteristics from the fundamental aspect, such as the existence of interface, the large difference in the thickness and the mismatch of the mechanical properties between the film and substrate material. These characteristics make the failure mechanism of the film/substrate system very special.[12] In the present work, we study the formation and propagation of the highly ordered wavy cracks in sol-gel silica films deposited on silicon or glass substrates with different dimensions. A model considering the coupling of two different kinds of crack modes is proposed to interpret the wavy crack path and correlated with the dynamic propagation process. The stress evolution along the crack path is discussed and evaluated based on this model. It is also interesting to find that the dimension of the wavelength and the amplitude are well governed by the scaling laws which were not found before in this system.

II. EXPERIMENT

The sol-gel process was used to deposit the films on substrate. In a typical process, tetraethyl orthosilicate (TEOS), water and ethanol were mixed with the concentration of TEOS around 0.2 M and the volume ratio between water and ethanol was around 1:3. The mixture was stirred for half an hour and then the diluted HCl (0.01 M) was added to adjust the PH=2. The obtained mixture was transparent and clear without any precipitate, which was refluxed under continues stirring in 60 °C water bath for about 4 h to promote the polymerization of TEOS. The commercial glass slide used in microscopy or the silicon wafer Si(100) cleaned by a standard RCA process was used as substrate for film deposition. The glass slide was first washed by a mixture of $NH_3 \cdot H_2O$, H_2O_2, and deionized water, and followed by dipped into the 4% hydrofluoric acid for several seconds.

The spin-coating method was used to prepare silica thin films with a typical speed of 3000 rpm. The typical thickness of the silica films is ranged from 400 nm to 550 nm as measured by using a scanning electron microscopy (SEM, XL30, and FEI). After settling the as-deposited films for several seconds in air, flowing hot air with temperature around 40 °C was blow onto the film surface. Tension stress grows soon after the film was deposited onto the substrate and followed by heating with the hot air.[11] Different kinds of crack patterns can be observed after hot-air heating for several seconds when the tension stress grows to a critical value. The crack patterns on the film surface were observed by using an optical microscopy equipped with a charge coupled device camera. The morphology of the crack is studied by using an atomic-force microscopy (AFM, Nanoscope IIIa, and Veeco) with contact mode.

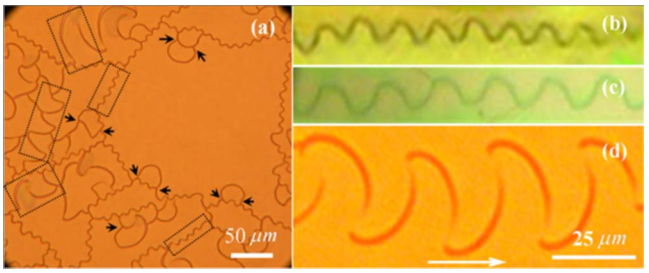

FIG. 1. (Color online) Optical microscope images of wavy cracks with (a) large area and the wavy cracks with different wavelength ranging from (b) several microns to [(c) and (d)] several tens of microns. The arrows in (a) indicate the secondary cracks initiated perpendicular to the first crack path. Rectangles indicate the wavy cracks with different dimensions near to each other.

III. RESULTS AND DISCUSSIONS

Typical morphology of the cracks in the silica films deposited on substrate is shown in Fig. 1(a). Different kinds of cracks could be found in the figure. Most of the cracks have arclike path that distributed randomly on the surface. Typically, some oscillated wavy cracks with length of more than 100 μm are easy to be observed. They are distributed randomly on the film surface and connect with each other. It is found that the cracks are nonsensitive to the heating direction of the hot air. Isotropically distributed cracks could be found in the directional heating conditions. The cracks are not created at the same time during the process, secondary cracks could be observed that initiated from the previously created cracks. Several initials of the secondary cracks are marked by the arrows in the figure. It is found that the propagation direction of the secondary crack is always nearly perpendicular to the first created crack at the initial site. Wavy cracks with distinct dimension are observed even adjacent to each other as indicated by rectangular shape, implying that the dimension of the cracks is not directly determined by the film thickness. Similar scenario can be also observed in films with different thickness, which further argues that the dimension of the cracks have little dependence on the film thickness. Several typical morphologies of the ordered wavy crack with different dimensions are presented in Fig. 1(b)–1(d) and the arrow in Fig. 1(d) shows the crack propagation direction. Detailed observation shows that the path is not sinusoidal like, kinks could be always observed along the crack trajectory, which is similar to the situation described in Refs. 4 and 9.

One of the typical morphology of the wavy cracks with the kinks observed by using AFM is presented in Fig. 2(a). Here, the nonsinusoidal-like wavy crack path is more obvious. There are two arclike curves in each period of the crack path, and sharp kinks exist between the two adjacent smooth arclike curves. Two sequences of serration leaves can be observed along the crack path that separated is by a crack gap. The formation of the crack gap between the two crack edges indicates the part of the film aside the crack line is greatly deformed in the in-plane directions. It is found that the width of the crack gap between the two crack edges is not constant, which indicates that the deformation extent of the serration

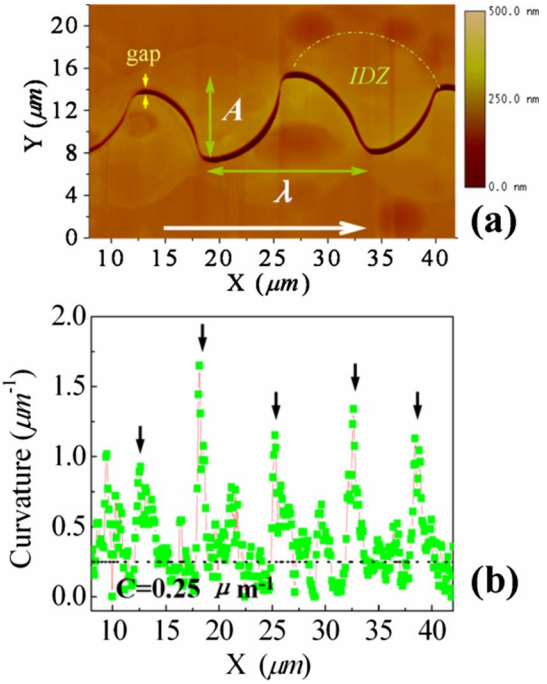

FIG. 2. (Color online) (a) An AFM microscope image of a wavy crack on silicon substrate, marked with the wavelength and the amplitude. IDZ stands for the interface debonded zone, one of which is denoted by dashed line. The gap between the two crack edges is indicated by yellow arrows. (b) The corresponding curvature changes along the crack path, where arrows indicate the kinks and the dashed line indicates the C=0.25 line.

leaves is different along the crack trajectory. It is also found that the cusps of the serration leaves at each crack side have larger plastic deformation than that at the valleys. Some circular areas are clearly identified around the crack lips aside the serration leaves. The AFM-depth analyze found that some surface protuberance occurs in the circular areas and the maximum protuberance observed is about 12 nm, which is about ~2% in respect to the film thickness. This small protuberance may resulted from the effect of the in-plane stress accumulation during film-cracking process according to the von-Karman plate theory,[13] which means that the circular areas with different contrast observed here are the part of the film debonded from the substrate.

In order to see the detailed shape change along the wavy crack path, the crack path shown in Fig. 2(a) is digitalized and the curvature (C) that related with the direction change is obtained and presented in Fig. 2(b). As seen in the figure, although the curvature along the crack path changes from site to site, most of the data points were distributed aside the dashed C=0.25 line as indicated in the figure. This result indicates that the crack path is in fact composited by quite regular arc-shaped segments. The arrows in the figure indicate the evidently larger curvature at the kinks, which indicates the abrupt change in propagation direction at these points. Analyzing about some other cracks with different dimension also shows the similar characteristic that the crack trajectory is composited by the smooth part and the kink part. It is needed to be noted here that the kink angle, which describes the change in the propagation direction at the kink,

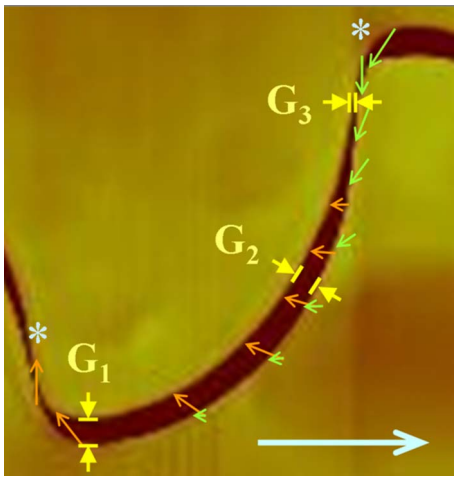

FIG. 3. (Color online) The anticipate deformation and shift of the serration leaves along the wavy crack. The orange and green arrows indicate the deformation shift of the two adjacent crack leaves. Different places have different shift, indicating different dynamic process. G_{1-3} stands for three gaps with different widths.

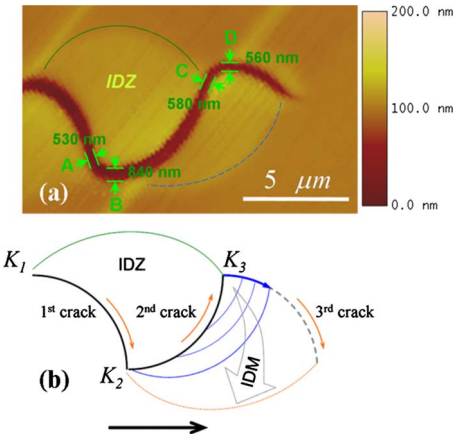

FIG. 4. (Color online) (a) An AFM microscope image shows the uncompleted crack tip with the stress region formed after the second crack and the different width of the crack gap. (b) The model illustrating the crack propagation process and the stress zone evolution in the wavy cracks. $K_{1\sim3}$ stands for the kinks. Dashed lines indicate the suppositional process, arrows indicate the propagation directions.

is not constant in cracks with different dimensions, and it is distributed in the range of about 60°–160°. According to our observations, cracks with larger dimensions show smaller kink angle and smaller cracks have larger kink angle. The wavy cracks with larger kink angle show the trajectory similar to the sine-shaped curve, in which the characteristic of kink is less pronounced and the smooth part cannot totally descript by a serious of arc-shaped segments.

According to the previous reports, it is realized that the formation of the curved crack path in the film (plane-stress state) could be caused by the mixed loading state of types I and II at the crack tip during the dynamic propagation process, where the type I loading refers to the loading force point to the direction perpendicular to the crack tip, while type II loading refers to the loading force point to the direction parallel to the crack tip. The principle of local symmetry indicates that the crack tip will change the propagate direction in order to sustain the type I style in vicinity of type II loading.[14] As a result, the change of the ratio between K_I/K_{II} can be used to interpret the curved crack path. As the in-plane deformation and shift is directly related with the stress evolution in the film, here we try to interpret the origin and the evolution of the types I and II stress loading by analyzing the deformation and shift of the serration leaves along the crack path.

Figure 3 gives the detailed analyze about the width of the gap and the anticipated deformation of the film along one of the crack periods. The width of the gap changes at different sites of the crack leafs due to different deformation extent of the two crack leaves. For example, the gap G_1 that near the kink has the largest width, while the gap G_3 has the smallest width, and the gap G_2 between them has the medium width. The anticipated shift of the upper and lower part of the crack leaves is indicated by orange and green arrows, respectively. For the upper crack leaf, the shift near the tip (near G_1) is mainly along the direction normal to the propagation direction. The lower crack leaf have relatively smaller shift because it is bonded with the substrate there so the gap G_1 is mainly caused by the transverse shift of the upper leaf and it is seemed to be type I because the crack direction is perpendicular to the shift of the crack leaves. Similar situation appears at the site near the tip of the lower crack leaf (near G_3), where the small gap is caused by the transverse shift of the lower crack leaf, as the crack is formed along the same direction with the shift of the crack leaves, it is realized to be type II. For the smooth part between these two sites, the upper crack leaf show gradually decreasing shift along the crack propagation direction and the deformation shift changes from normal to parallel direction, so the gap G_2 can be realized as the mixture of types I and II. Based on the above discussions, it is concluded that the deformation and the in-plane shift of the debonded part of the film is the source of the types I and II stress loaded on the crack tip.

It is a good way to study the dynamic process by observation the propagation of the crack directly. From another aspect, it can be also well interpreted by analyzing the wavy crack path. An AFM micrograph shows a crack with an unfinished end is presented in Fig. 4(a), where the uncompleted crack and the circular shaped debonding area could be clearly resolved. The arclike crack curves and the debonded circular areas are also well resolved similar to Fig. 2(a). The debonded area (noted by solid, green line) along the unfinished crack curve is different from that along the finished crack curves (noted by dashed, orange line) as indicated in the figure, which indicates that the debonding of the films is occurred gradually and simultaneously with the crack of the film during the crack propagation process. The width of the crack gap at several special points (similar to G_1 and G_3) noted as A (530 nm), B (840 nm), C (580 nm), and D (560 nm) are also shown in the figure, where sites A and B are located on the finished crack circle, sites C and D are located on the unfinished crack circle. It is found that gap B is evidently wider than the gap D while gap A is relatively narrower than gap C. We attribute these differences to the se-

quential interface debonding and film deformation and shifting during the propagation process, which means that the part of the debonded film will shift aside gradually in different manner (type I or type II) under different extent during the crack process considering that only the part of the debonded film can deform and shift. As the interface debonding is the prerequisite of the deformation and shifting of the film, only the part of the debonded film will apply additional stress upon the crack tip, and which is realized to be the source of the types I and II loading that mentioned previously. Based on this idea, it is estimated that the tangent stress gets the maximum when the crack tip approaches to the kink, and the shift of the part of the film near to the kink is mainly along the tangent direction (type II). After passed the kink, the crack propagates along the deviated direction respect to the previous circular crack leaf, now the stress is in fact turn to be type I. Between the adjacent two kinks, the mixed loading of types I and II stress is raised from the deformation of the debonded film in directions both along and perpendicular to the crack path. During the crack propagation process, the crack mode changes gradually from type I to type II in the circular segment and then changes abruptly back to type I at the kink.

A schematic model demonstrates the propagation of the wavy crack is drawn in Fig. 4(b) according to the observation in Fig. 4(a). There are several considerations during construction the current model: (1) if the part of the film is bonded with the substrate, then there will be little in-plane deformation, so it is realized that the interface debonding must occur before the in-plane deformation; (2) crack of the film is also the precondition for the in-plane deformation, or there will be no crack gap formed; (3) the deformation in the part of the debonded film will affect the stress state at the crack tip, so the shape and area of the debonded part of the film is strongly correlated with the crack path; (4) the debonding zone is determined directly by observing the debonded circular area in the AFM image. Based on the above points, the dynamic cracking process can be interpreted from the steady-state AFM image. As shown in the figure, the first and second cracks occur in a circular manner, with a kink between them (K_1). The interface debonding zone (IDZ) along the circular crack halves, with a circular shape, are also shown. The third unfinished circular-crack half begins after the second kink (K_2). During the third crack propagating, the interface debonding mode is performing simultaneously. It seems that the third crack will propagate until a kink is reached and then the similar process occurs again. Here, the interface debonding is coupled with the film crack, and the stress distribution around the crack tip is affected by the part of the debonded film, which gives rise to the mixed stress state at around the crack tip and make the crack tip propagates in a circular style. It is also noted that in the dynamic propagation process, the crack trajectory, especially at around the kinks, will be affected by the dynamic effect that related with the propagation velocity, as a result the characteristics of the kinks and the circular shape will be less pronounced.

As the interaction and coupling is in fact the stress field evolution around the crack tip, it is convenient to interpret the crack process by employing the infinite elementary

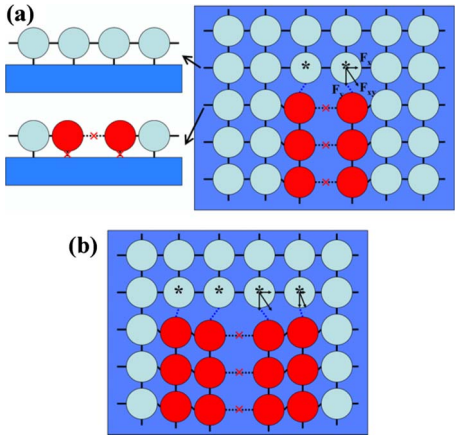

FIG. 5. (Color online) The infinite element model of the crack in thin film deposited on substrate. (a) Right part: plane view of a crack in film deposited on substrate, and left part: cross-sectional view of the unit ahead (upper part) and below (lower part) the crack tip. (b) Plane view of a crack with extended debonded part of the film, which indicates that the propagate velocity ratio of the interface debonding and film crack is larger with respect to that in the situation shown in figure (a). Red circles stand for the debonded units with the substrate, dashed lines with a red cross are the bonds broken, and blue lines at the crack tip are the stressed bonds. The arrows denoted on the units at the crack tip show the forces or partial forces which have the similar meaning with that shown in (a).

model as shown in Fig. 5(a), where the film is divided into many small unit (circles) that connected with each other by the springs (short lines). The effect of the interface bonding is also described as the spring. The typical scenario after create one crack line in the film is shown in the right part in Fig. 5(a), where the crack propagates as the sequence broken of the spring: film is broken as a result of the broken of the horizontal bonds that connect the adjacent units and the interface is debonded as a result of the broken of the perpendicular bonds that connect the substrate and the film. The red crosses on the dashed bonds indicate the broken bonds that form the crack path. The units in red indicate that they are debonded with the substrate. The corresponding cross-sectional view is also shown in the left part in Fig. 5(a), where the upper image shows the part of the film without any crack and the lower part is the part of the cracked film as indicated by the arrows. As the film is tensor stressed before crack, the debonded units will shift aside from the direction that perpendicular to the crack line after the crack created. Due to the shift of the units, the two bonds (dashed) at the crack tip is stress accumulated. The units at the tip (marked as asterisks) will be under the stress of F_{xy} as depicted in the figure, which can be divided into two partial force as F_x and F_y, where F_x can be realized as type I loading and F_y can be realized as type II loading. Due to the coexistence of the mixed stress at the crack tip, the propagation direction will be changed.[14]

Since both the partial forces are related with the debonded area of the film: the larger the debonded area, the larger the deformation, and the larger the partial forces, it is realized that if the debonded area is large enough, considerable type

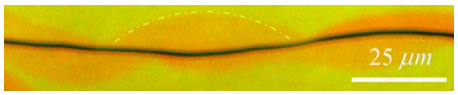

FIG. 6. (Color online) Optical microscopy image shows a slightly curved straight crack with the debonded area around the crack line. Dashed line indicates one of the debonded areas.

II stress accumulation will occur at the crack tips, which will result relatively larger change in the crack propagation direction. This situation can be interpreted from Fig. 5(b), where the debonded part of the film is relatively larger, as a result the type II loading is relatively larger. It is also considered that if the type II stress accumulation is large enough, the change in the propagation direction will accompanied with the crack mode changes from type I to type II, which can be used to understand the situation at the site of G_3 at the kink. We note that if type II stress is large enough, the bond broken can also be occurred among the bonds parallel with the propagation direction, which will results the new created crack propagates along the transverse direction. In this case, the formation and propagation of the transverse crack is also performed in expend of the type II stress, but in fact it is the type I nature, which is the situation at the site of G_1. The above process can be used to interpret the crossover of the crack mode from type II to type I at the kink. Based on the proposed process, the kink angle is in fact determined by many factors such as the stress state at the crack tip, the dynamic behavior and the material properties, etc. Here we attribute the change in the kink angle mainly to the dynamic effect caused by the stress evolution and film-deformation process, which can be interpreted based on the fact that the big cracks propagates with relatively slower velocity and results relatively smaller kink angle, while vice versa.[15] In other cases, if the stress singularity occurs along the crack path after the crack tip, the secondary cracks will initiate from the edge of the crack path. This situation is easy to be interpreted from Fig. 5 that the secondary crack is initiate normal to the primary crack edge, which is just like the sites indicated by the arrows in Fig. 1(a).

It is meaningful to analogy the current kinked wavy cracks with the highly nonsinusoidal trajectory reported previously in Refs. 4 and 10 despite very different loading conditions and geometry. And it is also suggested that the stress evolution during these kinds of bifurcations can be considered for thoroughly understanding the dynamic process.

As a matter of fact, the debonding of the film could be also found around the straight or the slightly curved cracks in most of the experiments. Figure 6 gives one of the typical slightly curved cracks. The shaded area indicated by dashed line around the crack path is confirmed to be the part of the debonded film by using AFM measurement that is similar to the situation discussed in Figs. 2(a) and 4(a). According to our *in situ* observations, the straight cracks have evidently larger propagation velocity than that for the wavy cracks and the cracks with larger wavelength and amplitude always have relatively slower propagation velocity.[15] As mentioned above, the wavelength and the amplitude of the wavy path show little dependence on the film thickness, here it is suggested that the formation of the wavy cracks is more favored to be governed by the propagation velocity. It is noted that although the interaction of the interface debonding and the film crack has been discussed by several researches,[16–18] the effect of the propagation velocity on the interaction and coupling are not discussed. Here we try to illustrate this point based on the above experimental results.

It is reasonable that the overlap both in the time and space domain is the preconditions for the interaction and coupling between the two kinds of crack. If they are far away from each other or they happen with the relatively longer time interval, the interaction and coupling is less probable to happen. For the two kinds of cracks discussed here, we note that they happen to be both in the coincident place and time, so they are easy to interact and couple with each other as discussed in Figs. 5(a) and 5(b). Although the interactions are easy to be occurred, for dynamic cracks, due to the velocity difference in the film crack and interface debonding, the debonded area that is just below the propagation crack tip will be different, as a result the interaction or coupling strength will be different. Considering the interface debonding had a relatively larger velocity (or equally, the film crack have relatively smaller velocity), the new created debonded area will be relatively larger at the same interval time, which will result in larger type II stress loading at the crack tip and the propagation of the crack will be occurred. This situation can be interpreted by comparing the situations depicted in Figs. 5(a) and 5(b). In the opposite manner, if the interface debonding is much slower than the propagation of the film crack (or equally, the film crack have relatively larger velocity), the crack process of the film will be less affected by the interface debonding, which can be used to interpret the situation shown in Fig. 6, where the debonded part of the film seemed to be mainly created after the crack of the film.

We note here the detailed relationship concerning the propagation velocity and the wavelength or amplitude must resort to the computer simulation, where the bond parameter such as the spring's strength constant and the critical broken force can be tuned systematically. So that the dynamic process in formation of the wavy cracks can be tracked and the critical conditions for formation of the wavy cracks can be obtained.

As the wavelength and the amplitude are more likely dependent on the crack velocity than on the film thickness according to our observations, it is interesting to find that if there is any quantitative relationship between them. By surveying 448 pieces of crack lines, the wavelength and the amplitude of the wavy path are obtained and a log-log plot of them is presented in Fig. 7. It is found that the power-law relationship can be used to best describe the relationship as

$$\lambda \sim A^{\xi}, \tag{1}$$

where λ stands for the wavelength, A stands for the amplitude, and ξ is the scaling factor. A least standard-deviation fit of the data points gives out $\xi = 0.47 \pm 0.01$ as appeared as the line shown in the figure. The existence of the scaling property uncovers the self-affine nature in the wavy cracks. Similar to the situation discussed in Refs. 19 and 20, the scaling properties discussed in these kinds of fractures in fact deal with the fluctuation of the crack surface, i.e., the rela-

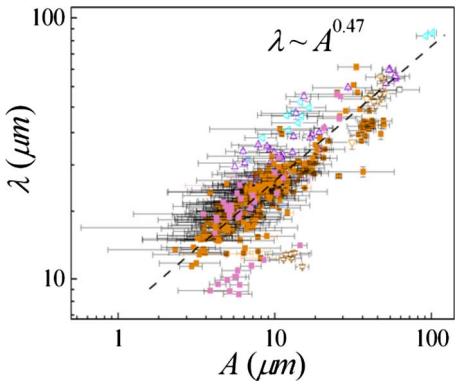

FIG. 7. (Color online) The log-log plot of the amplitude versus wavelength, which suggests the scaling rule. This figure includes totally 448 pairs datum obtained from the digitalized wavy patterns; and dashed line is the best linear fit performed with a least standard deviation method. In order to separate the data points obtained from different samples, some of the data points corresponding to the cracks in the same sample are appeared as the same marks. Typically, the filled pink rectangle and the hollow yellow triangle corresponding to cracks in two samples, which have "special points" that is evidently deviated from the fitting line. As both the special points and the "normal points" are presented in the same sample, we suggest that the deviated points are not caused by the different film thickness, but are more favored to be related with the properties of the crack itself.

tionship between the perturbation perpendicular to the crack path and the characteristic dimension along the crack path. The universal properties observed indicating that although the surface instabilities is involved during the cracking process,[21] the crack surface [three-dimensional (3D) situation] or crack path [two-dimensional (2D) situation] is essentially governed by the self-organized nature. We note that similar to the periodical crack path presented in the quasi-2D system here, the periodical crack morphologies have been reported by many researches in the 3D systems,[22] which indicate the analogical situation.

From another hand, it is noted that the scaling factor observed here is much smaller than previous results, which suggests there may have some particularities in the current situation. It is suggested that the situations previously reported were evaluated in the 3D situation and the scaling properties were revealed in the 2D fracture surface while in the current case the crack is performed in the quasi-2D system and the scaling properties is in the one-dimensional situation. The change in the dimension in the current system could probably the reason for smaller scaling factor.[22] In a word, the observation of the scaling property indicates the fundamental self-assemble nature in the ordered cracks. It is emphasized that both the dimension and the shape are well organized in the process while the stress evolution were the key factor in controlling the crack path.

IV. CONCLUSION

In conclusion, wavy crack with a scaling-property relationship between the wavelength and the amplitude is observed in the quasi-2D silica films. The observation of the scaling property indicates the highly ordered self-assemble nature during the cracking process. The wavy crack path is realized to be resulted from the coupling of the film crack and the interface delaminate mode when their velocities are comparable with each other. The coexistence of the types I and II stress governs the crack propagating process. The types I and II loading at the crack tip during the crack propagation are resulted from the part of the film debonded with the substrate, which is the key fact in the formation of the wavy crack path.

ACKNOWLEDGMENTS

This work is supported by NSF of China (Grants No. 10874070 and No. 60721063) and "973" project (Grant No. 2007CB613401) and SRFDP (Grant No. 20070284020).

*Corresponding author; junxu@nju.edu.cn

[1] A. J. Rosakis, O. Samudrala, and D. Coker, Science **284**, 1337 (1999).
[2] E. Sharon, S. P. Gross, and J. Fineberg, Phys. Rev. Lett. **76**, 2117 (1996).
[3] R. D. Deegan, P. J. Petersan, M. Marder, and H. L. Swinney, Phys. Rev. Lett. **88**, 014304 (2001).
[4] A. Yuse and M. Sano, Nature (London) **362**, 329 (1993); see also, R. D. Deegan, S. Chheda, L. Patel, M. Marder, H. L. Swinney, J. Kim, and A. de Lozanne, Phys. Rev. E **67**, 066209 (2003).
[5] M. Adda-Bedia and Y. Pomeau, Phys. Rev. E **52**, 4105 (1995).
[6] S. Yoneyama, K. Sakaue, H. Kikuta, and M. Takashi, Exp. Mech. **48**, 367 (2008).
[7] H. A. Bahr, A. Gerbatsch, U. Bahr, and H. J. Weiss, Phys. Rev. E **52**, 240 (1995).
[8] Y. Sumi and Y. Mu, Mech. Mater. **32**, 531 (2000).
[9] F. Corson, M. Adda-Bedia, H. Henry, and E. Katzav, arXiv:0801.2101 (unpublished).
[10] B. Audoly, P. M. Reis, and B. Roman, Phys. Rev. Lett. **95**, 025502 (2005).
[11] M. Sendova and K. Willis, Appl. Phys. A **76**, 957 (2003).
[12] Z. C. Xia and J. W. Hutchinson, J. Mech. Phys. Solids **48**, 1107 (2000), and the references therein.
[13] A. A. Abdallah, D. Kozodaev, P. C. P. Bouten, J. M. J. Toonder, U. S. Schubert, and G. With, Thin Solid Films **503**, 167 (2006).
[14] T. Fan, *Fundamental of Fracture Theory*, 1st ed. (Science, Beijing, China, 2003).
[15] Although detailed results still lack in the current stage, the obvious effect has been observed *in situ* during the experiment: quick crack always results in the crack sequence with much small wavelength and amplitude while slow cracks always results in large wavelength and amplitude.
[16] S. Kitsunezaki, Phys. Rev. E **60**, 6449 (1999).

[17] A. Nakahara and Y. Matsuo, Phys. Rev. E **74**, 045102(R) (2006).
[18] S. Sadhukhan, J. Prehl, P. Blaudeck, K. H. Hoffmann, T. Dutta, and S. Tarafdar, arXiv:0805.2779 (unpublished).
[19] L. Ponson, D. Bonamy, and E. Bouchaud, Phys. Rev. Lett. **96**, 035506 (2006).
[20] S. Morel, J. Schmittbuhl, E. Bouchaud, and G. Valentin, Phys. Rev. Lett. **85**, 1678 (2000).
[21] See, for example, E. A. Brener and V. I. Marchenko, Phys. Rev. Lett. **81**, 5141 (1998).
[22] See, for example, S. J. Kwon, J. H. Park, and J. G. Park, Phys. Rev. E **71**, 011604 (2005); V. Shenoy and A. Sharma, Phys. Rev. Lett., **86**, 119 (2001); G. Wang, D. Q. Zhao, H. Y. Bai, M. X. Pan, A. L. Xia, B. S. Han, X. K. Xi, Y. Wu, and W. H. Wang, *ibid.* **98**, 235501 (2007), and the references therein.